INT. J. REMOTE SENSING, 2002, VOL. 23, NO. 19, 3959–3970

Taylor & Francis
Taylor & Francis Group

Desert scrub optical density and spectral-albedo ratios of impacted-to-protected areas by model inversion

J. OTTERMAN†, A. KARNIELI‡, T. BRAKKE§, D. KOSLOWSKY¶, H.-J. BOLLE¶, D. STARR†† and H. SCHMIDT‡

†Land-Atmosphere-Ocean-Research (LAOR), Data Assimilation Office, NASA/GSFC Code 910.4, Greenbelt, MD, 20771, USA
‡Desert Research Institute, Sede Boker, Israel
§Biospheric Sciences Branch, NASA/GSFC, Greenbelt, MD, 20771, USA; e-mail: tbrakke@ltpmail.gsfc.nasa.gov
¶Berlin Free University, Carl-Heinrich-Beckes-Weg 6-10, 12165 Berlin, Germany; e-mail: KOSZE@ZEDAT.FU-berlin.de
††Atmospheric Sciences Branch, NASA/GSFC, Greenbelt, MD, 20771, USA

Abstract. Bidirectional surface reflectances measured from NOAA AVHRR over the Negev (southern Israel) and the Sinai are analysed to assess the impact on the surface characteristics of anthropogenic pressures of overgrazing. The impacted Sinai is assumed bare, while the Negev is vegetated by desert scrub. The Negev plants are known to be much darker than the underlying soil, and thus assumed to be absorbing (black). The leaf area distribution as a function of the zenith angle is modelled initially as that of small spheres, which specifies a pronouncedly vertical architecture. We infer from the Negev-to-Sinai reflectance ratios the optical thickness τ_b of the plants (spheres) in the range 0.12 to 0.20 for channel 1 (band centre at 0.63 μm), with only weak seasonal variability. Evaluated from average values of τ_b, the Negev-to-Sinai ratios of the spectral albedos (hemispheric reflectances) are 0.63 and 0.55 in channel 1 and 0.67 and 0.60 in channel 2, at solar zenith angles of 30° and 60°, respectively. These ratios indicate the severe climatic impact of overgrazing in the Sinai, inasmuch as a high albedo means reduced shortwave heat absorption (which is detrimental to rainfall-inducing convection). We subsequently proceed to invert the Negev-to-Sinai reflectance ratios assuming a plant-element distribution tending even more to the vertical. The values of τ_b are reduced when derived for a greater tendency to vertical architecture. The Negev-to-Sinai ratios of the spectral albedos are also significantly lower in these cases, which means that the assessed impact of overgrazing in the Sinai is indeed extremely severe. We conclude that plant architecture (which controls the reflection anisotropy) should be considered when evaluating the albedos of vegetated versus bare (impacted) surfaces from satellite-measured bidirectional reflectances. Uncertainty in the zenith angle distribution of the leaf area produces significant uncertainty in the albedo assessment. Multidirectional reflectance measurements made near the ground would greatly reduce uncertainties about the surface-reflection anisotropy, and thus enhance the value of satellite measurements.

Paper presented at an International Workshop on 'Land Cover/Land Use Change and Water Management in Arid Regions: Remote Sensing Applications in the East'. The workshop took place at the Jacob Blaustein Institute for Desert Research, Sede Boker Campus, Ben Gurion University of the Negev between 23–27 October, 2000.

International Journal of Remote Sensing
ISSN 0143-1161 print/ISSN 1366-5901 online © 2002 Taylor & Francis Ltd
http://www.tandf.co.uk/journals
DOI: 10.1080/01431160110115753

1. Introduction

In an interesting recent study of surface characteristics, researchers at the Jacob Blaustein Institute for Desert Research of the Ben-Gurion University (Sede Boker Campus in Israel) analysed seasonal vegetation dynamics by calculating from Landsat data the Vegetation Index (essentially, the ratio of the reflectance in the infrared part of the solar spectrum, 0.7–1.2 μm, to that in the visible (red) band, wavelengths below 0.7 μm) along a north-to-south transect in Israel from the Galilee in the north, to the northern Negev in the south (but not into the Sinai, beyond the Negev). The increases in the Index during the growing season indicate the increased density of the plant cover. Thus, the Vegetation Index has proved itself once more to be a pertinent tool for assessing green plant density and crop vigour, just as it has in many studies of Landsat data. Indeed, band selection for the Landsat Multispectral Scanner System (MSS) was based on the well-established finding that green plants absorb strongly in the red band (low reflectance, mainly because of the chlorophyll absorption), but predominantly scatter (high reflectance) in the solar infrared (Breece and Holmes 1971, Blad and Baker 1972, Colwell 1974, Bunnik 1978).

The Vegetation Index is not an appropriate measure, however, of the natural plant cover in arid areas where precipitation is below 250 mm y^{-1}. Sparse plant cover, called desert scrub, which grows under low moisture conditions, consists only of species that survive the dry season with minimal evapotranspiration. The prophet Jeremiah's description (Chapter 2, Verse 2), '... in the desert, in the land not sown,' is a pertinent definition of such regions. Hunting or grazing (under nomadic practices) is possible, but not conventional agriculture (the Biblical term *midbar*, usually translated as desert, but sometimes as wilderness, implies grazing land). The flora of the Negev and the *much* sparser flora (as a result of overgrazing and gathering of plants for firewood) of the northern Sinai are both described by Otterman *et al.* (1975).

Desert scrub is much darker than the underlying soil in the visible (see the photographs of the steppe regions in Dregne, 1970), *and* also in the infrared spectrum, as is shown in analyses from MSS measurements over the bright, overgrazed Sinai and the much darker Negev that was protected from overgrazing (for the initial study by microdensitometer of MSS black-and-white transparencies, see Otterman (1974); for more accurate calculations, from MSS digital tapes, see Otterman and Fraser (1976)). The Negev-to-Sinai reflectance ratios in any MSS spectral band conveniently quantify the spatial difference produced by anthropogenic impact (but comparing *hemispheric* reflectances is more appropriate for climate-related studies, see later discussion). The ratios are surprisingly similar in each band, so taking a broad-band average is also a reasonable quantifier of the impact. This type of measurement was used to assess a *temporal* change in the surface albedo by Courel *et al.* (1984), who analysed the change that occurred in the Sahel (fringe region of the Sahara) between satellite passes approximately six years apart.

The Landsat MSS scans through a small angle only, and thus the measured reflectances can be approximately regarded as taken from the zenith, that is, as nadir reflectances. Reflectances measured from Landsat are commonly used for detection of change in the surface (Courel *et al.* 1984). For isotropic (Lambertian) surfaces the reflectance does not depend on viewing/illumination geometry. For such surfaces, off-zenith reflectances (now available from NOAA Advanced High Resolution Radiometer, AVHRR) are equivalent to the nadir measurements, and likewise equivalent to the hemispheric reflectances (spectral albedos). For anisotropic surfaces, nadir reflectance is directly useful as change-detection parameter only as long as the solar zenith angle does not change significantly (cloudless conditions are implied).

Significant anisotropy can characterize bare desert sands (Coulson 1966, Coulson and Reynolds 1971, Pinty *et al.* 1989) as well as desert scrub surfaces (Deering *et al.* 1993). For a bare sandy surface, the hemispheric average tends to be *higher* than the nadir reflectance because of pronounced backscattering (reflection into the solar quadrant; this effect is smoothed-out for coarse-resolution reflectances of undulating sands). Conversely, for a desert scrub surface, the hemispheric average is *lower* than the nadir reflectance because the very dark, predominantly vertical plants intercept the rays reflected from the soil off-zenith more strongly. Thus, the Negev-to-Sinai nadir-reflectance ratios, measured by Otterman (1974) and Otterman and Fraser (1976), as well as the ratios for the border areas in the former Soviet Union, protected from overgrazing, to the overgrazed Afganistan (see Otterman 1981a), underestimated the ratio of the hemispheric reflectances. This problem of surface anisotropy is addressed in our present study by analysing bidirectional (off-zenith) reflectances measured by AVHRR.

The AVHRR measurements provide the capability to assess reflectance anisotropy as demonstrated by Koslowsky (1996, 1998), inasmuch as data are available for a range of view directions and zenith-angles of solar illumination. Koslowsky's main interest was to convert off-zenith view data to nadir reflectances to be used as change-detection indicators. By this approach, the nadir-correction factor was compiled for desert areas, the Tuscany region in Italy, the Iberian Peninsula, and some regions in mid-Europe.

We apply here the anisotropy information to derive ratios of *hemispheric* reflectances. Lack of information about reflection at large-zenith angles prevents a truly accurate determination, as discussed by Kimes and Sellers (1985) and Otterman (1985). We present here a new model for the desert scrub canopy, which is applied to assess uncertainties that arise when the canopy architecture is not known.

2. Satellite data preprocessing

The present study is based on NOAA-14 AVHRR satellite data, which were transmitted to the receiving station in Sede Boker (Negev, Israel) in the afternoon (around 13:30). The satellite images were received in High-Resolution Picture Transmission (HPRT) format: 10-bit precision, and 1.1 km spatial resolution at nadir. NOAA-14 AVHRR images of Israel were obtained for the two-year time period from June 1995 to April 1997.

The study areas were extracted from all the available images that fulfill a certain quality requirement, for example, 'cloud-free'. The distortion introduced by the extreme scan angle was reduced by limiting the use of the images to the satellite zenith angles within 30° of the nadir. The entire processed time period is represented by several images per month.

The major problem of any analysis of AVHRR data is the lack of radiometric calibration on board. The high slant angle, which distorts radiometric observations at off-nadir angles, makes atmospheric correction highly important. These factors have to be considered in order to get relevant results about the spectral properties of the Earth's surface.

For a detailed application of AVHRR data, the raw AVHRR 10-bit digital numbers (DN) must be converted into more meaningful physical quantities such as radiance and reflectance. Although the raw digital counts do provide some information about the relative behaviour of various surfaces (relative brightness), the 10-bit digital numbers must be converted to real physical parameters. This process of data

calibration of the visible and the near-infrared channel is based on calibration coefficients (Rao and Chen 1996). Within this study the pre-launch calibration coefficients or post-launch calibration algorithms were applied for the entire dataset.

This study applies the calibration procedure for channels 1 and 2 of the NOAA-14 AVHRR, based on the work of the group at the NOAA/NESDIS Office of Research Application (Rao and Chen 1996). The authors observed an upward trend in the 'slope' for both channels after the processing and analysis of AVHRR data from 10 years of a bright desert surface (Libyan Desert). This trend indicates a loss in sensitivity of the sensor instrument over time. Two calibration methods were applied and compared in order to study the influence of sensor degradation on geophysical products.

The radiance values calculated by use of the pre- and post-launch calibration coefficients represent only the 'top of atmosphere' (TOA) radiance. Rao and Chen (1998) revised their calibration (NOASIS internet release for NOAA 14 AVHRR users). This recalibration is quite important for 1998, but not substantial for the period of the study. Considering that we use *ratios* of reflectances, the discrepancy is not significant. The atmospheric correction was applied to both data sets with the different radiometric calibration. As mentioned above, NOAA/AVHRR data were acquired from the receiving station in Sede Boker. Data about the atmospheric condition during the acquisition of the AVHRR images were available from a ground meteorological station in Israel.

Estimates of total precipitable water and aerosol properties of the atmosphere were obtained from a CIMEL automatic tracking sunphotometer (Holben *et al.* 1998) installed in Sede Boker. The CIMEL sunphotometer has a 1.0-degree full angle field of view and measures with a frequency of 15 minutes. Movable filters are mounted in a rotating wheel. Standard filters located at 440, 670, 870 and 1020 nm are used for aerosol detection. An additional channel at 940 nm is used for measuring the water vapour content. The automatic tracking sunphotometer measured the radiance during the acquisition of the NOAA/AVHRR images.

Daily variations of atmosphere optical thickness are much higher than that of water vapour content. Consequently, in order to correct for atmospheric effects, one should measure the atmospheric variables exactly at the time of data acquisition. The automatic tracking sunphotometer met the above requirement. Sky radiance and atmospheric optical thickness were measured at the time of the NOAA/AVHRR image acquisition.

Atmospheric correction of the TOA reflectance was carried out using the Second Simulation of the Satellite Signal in the Solar Spectrum (6S) algorithm (Vermote *et al.* 1997). This computer program allows the estimation of the solar radiation backscattered by the Earth surface–atmosphere system, as it is observed by a satellite. For successful atmospheric correction, the code requires estimates of water vapour and aerosol content in the atmosphere. In this study, the following corrections were implemented for the AVHRR channels 1 and 2:

- Molecular correction—correction for Rayleigh scattering and absorption by stable gaseous constituents of the atmosphere (CO_2, O_2, O_3).
- Aerosol correction—correction for scattering and absorption by aerosols based on the aerosol optical depth at 550 nm.
- Water vapour correction—correction for absorption by water vapour in the near-infrared part of the spectrum based on the total precipitable water (cm) in the atmosphere.

The acquisition date (Sun-Earth distance), the solar zenith and azimuth angle, and the zenith and azimuth angle of the satellite describe the geometrical conditions for the satellite overpass.

Based on the CIMEL measurements during the acquisition of the AVHRR images, the water vapour content of the atmosphere could be specified. As well as this parameter, the ozone content of the atmosphere was entered in the model. With these parameters the program is required to compute the gaseous absorption and the Rayleigh component. The aerosol content is another important parameter. The new version of the code includes a desert aerosol model, which was used in this study. From CIMEL measurements, we were able to fix the aerosol content of the atmosphere by entering the aerosol optical thickness (τ) at the reference wavelength $\lambda = 550$ nm. Thus, we expect that our atmospheric correction is quite reliable. Considering that we analyse here the ratio of reflectances of two neighbouring scenes in the same frame, no appreciable errors are likely unless the atmosphere departs strongly from the plane-parallel assumption across the Negev/Sinai border.

The image data were geometrically corrected to a master image based on ground control points and applying a transformation second order. The accuracy of the correction lies at the subpixel level. The RMS error was plotted against the satellite zenith angle to determine the effect of off-nadir views on registration accuracy. The results show that the largest RMS errors are not associated with viewing geometry due to the fact that only images with a view angle less than 30° were analysed.

3. Inversion of the model

The present study is based on NOAA/AVHRR satellite data, with a spatial resolution of 1.1 km at nadir, received in Sede Boker almost daily. NOAA-14 AVHRR images of Israel were obtained for the two-year time period from June 1996 to June 1998. After pre-analysis, the Negev-to-Sinai reflectance ratios, R_n/R_e, were computed for each satellite pass in two AVHRR spectral bands: visible band 1 (0.63 μm band-centre) and infrared band 2 (0.85 μm band-centre); for details of AVHRR operation see Cracknell (1997). Since the Negev plant elements are by a factor of about four darker than the underlying sandy soil, we assume that the elements are non-reflecting, that is, absorbing (this involves some inaccuracy, which we accept here). While the desert scrub plants are characterized by a pronounced tendency to the vertical, a distribution $\sin i$ of the leaf area in the zenith angle I is assumed in this section (but a more general model, with a stronger or weaker tendency to the vertical architecture is analysed later). This distribution characterizes plant elements as small spheres, or alternatively, as very small planar leaves (fragments) scattered randomly in the canopy. After breaking up the spherical shells, we retain the original orientation of the fragments in the spherical shell.

From the R_n/R_e ratio we compute the plant optical thickness τ_b by inverting our model:

$$\frac{R_n}{R_e} = \exp(-\tau_b V) \tag{1}$$

where V quantifies the illumination/observation geometry, that is, the dependence of R_n/R_e on the solar zenith angle θ_o (we consider here only the direct solar beam) and the view zenith angle θ_v:

$$V(\theta_o, \theta_v) = \frac{1}{\cos\theta_o} + \frac{1}{\cos\theta_v} \tag{2}$$

This cosine dependence on θ_o and θ_v expresses the elongation of the path through the canopy with increasing zenith angle (more plant elements are encountered along a longer path). The term exp $(-\tau_b/\cos\theta_v)$ depicts in our model the increasing obscuration of the soil with increasing view zenith angle, the so-called limb-darkening of the desert scrub surface, a common characteristic of many steppe types when desert-bloom conditions do not apply (see Dregne 1970; also see figure 3 in Deering *et al.* 1993). The term exp $(-\tau_b/\cos\theta_o)$ expresses the shadowing of the soil from the direct beam, with sky radiance neglected.

The values of τ_b, derived from equation 1 and presented in table 1, are in each case lower in band 2 than in band 1. In general, absorption by plants is strong in the visible, whereas scattering predominates beyond 0.7 μm. However, the reduction in τ_b in band 2 as compared to band 1 (which we note in table 1) is quite small, unlike the decrease one would obtain for green vegetation, for which band 2 to band 1 difference in the optical thickness (when incorrectly inferred by an absorption

Table 1. The optical density of the Negev desert scrub computed for each satellite pass, assuming spherical leaf area distribution.

Date	θ_o (°)	R_n/R_e Ch 1	R_n/R_e Ch 2	τ_b Ch 1	τ_b Ch 2
6 July 1995	18.2	0.719	0.769	0.161	0.128
22 August 1995	21.4	0.695	0.735	0.173	0.146
30 August 1995	28.6	0.680	0.731	0.179	0.145
19 September 1995	31.7	0.634	0.694	0.206	0.165
28 September 1995	36.5	0.640	0.695	0.197	0.161
5 October 1995	42.9	0.677	0.735	0.154	0.122
17 October 1995	42.5	0.641	0.690	0.184	0.154
25 October 1995	48.6	0.654	0.703	0.169	0.140
5 November 1995	48.5	0.587	0.646	0.202	0.166
3 December 1995	59.4	0.623	0.658	0.152	0.134
21 December 1995	55.4	0.621	0.670	0.168	0.141
13 February 1996	47.2	0.654	0.686	0.172	0.152
29 March 1996	34.5	0.700	0.730	0.153	0.135
1 April 1996	28.5	0.646	0.672	0.193	0.175
8 April 1996	31.1	0.706	0.733	0.159	0.142
25 May 1996	21.9	0.706	0.726	0.167	0.154
12 June 1996	21.1	0.728	0.751	0.153	0.138
22 June 1996	19.5	0.708	0.723	0.166	0.156
1 July 1996	19.4	0.724	0.742	0.156	0.144
6 August 1996	23.5	0.730	0.748	0.150	0.138
15 August 1996	25.6	0.740	0.759	0.141	0.129
24 August 1996	28.4	0.755	0.771	0.129	0.119
12 September 1996	34.1	0.734	0.748	0.140	0.131
18 October 1996	48.1	0.715	0.731	0.131	0.122
4 December 1996	57.8	0.656	0.683	0.147	0.133
22 December 1996	58.6	0.686	0.710	0.129	0.117
9 January 1997	56.6	0.714	0.726	0.119	0.113
6 February 1997	50.1	0.700	0.748	0.139	0.113
7 February 1997	49.2	0.683	0.733	0.148	0.121
15 February 1997	47.5	0.718	0.774	0.134	0.103
16 February 1997	46.6	0.695	0.753	0.147	0.114
19 April 1997	31.3	0.687	0.797	0.165	0.100

model) would be very large. We conclude that the dark brown-grey shrubs of desert scrub absorb strongly in the infrared, only *slightly* less than in the visible.

The ratios presented in table 1 show considerable scatter. The R_n/R_e ratios and the values of τ_b are presented in figure 1 versus the date of satellite overpass. Notwithstanding the appreciable pass-to-pass scatter, we note the seasonal dependence. The seasonal variations that we expect are quite complex. The Sinai/Negev region is characterized by a steep gradient of precipitation, and thus in the December–February period the terrain is more likely to be moist (a darker soil) in the Negev than in the Sinai. Such moisture difference would produce lower R_n/R_e ratios and higher values of τ_b, which is indeed observed.

The Negev-to-Sinai spectral albedo ratio A_n/A_e is derived from the relationship

$$\rho_a(\theta_o)=\frac{A_n}{A_e}=2\int_0^{\pi/2}\exp\left[-\tau_b\left(\frac{1}{\cos\theta_o}+\frac{1}{\cos\theta_v}\right)\right]\cos\theta_v\sin\theta_v\,d\theta_v \qquad (3)$$

Evaluated from average values of τ_b, the Negev-to-Sinai ratios of the spectral albedos (hemispheric reflectances) are 0.63 and 0.55 in channel 1 and 0.67 and 0.60 in channel 2, at solar zenith angles of 30° and 60°, respectively. These ratios suggest severe climatic impact (by reduced absorption of insolation, and thus of associated convection) of overgrazing in the Sinai.

4. Inversion with model for variable architecture

We now proceed to invert the Negev-to-Sinai reflectance ratios assuming a plant-element distribution tending even more to the vertical than the spherical-shell distribution assumed in the previous section. Distribution of leaf area normals is such that the projection of the leaves increases with the zenith angle, so that shadowing

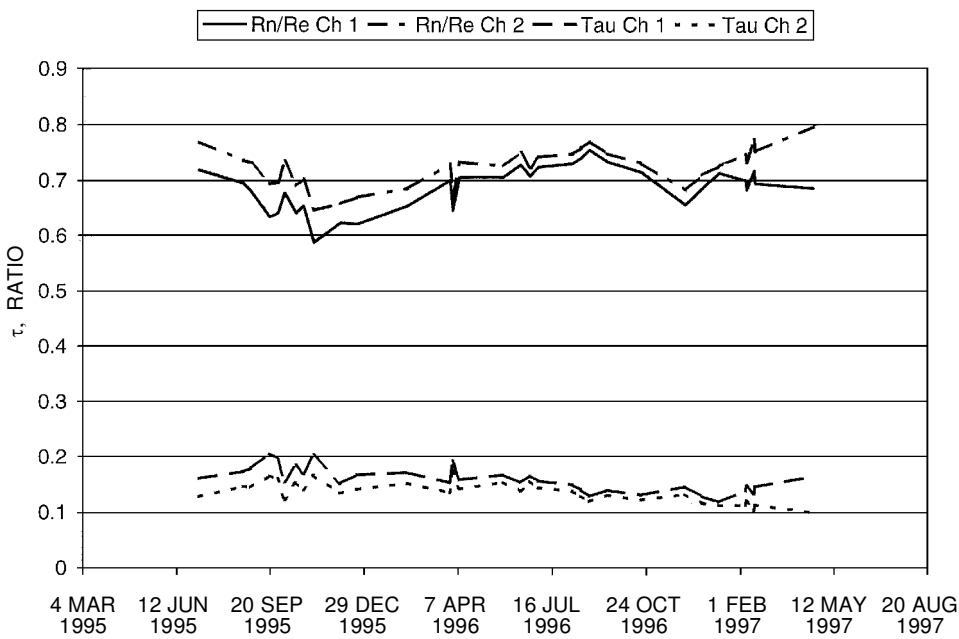

Figure 1. The Negev-to-Sinai bidirectional reflectance ratios, R_n/R_e, and the optical thickness τ_b inferred from these ratios, plotted versus the date of observation.

probability (per unit length of path) is proportional to $(\cos\theta_o)^{-z}$, and obscuration of the soil is similarly proportional to $(\cos\theta_v)^{-z}$, where z is our verticality parameter. In figure 2 we present graphs describing our new model for five different tendencies to the vertical. In figure 2 we plot the extinction by the canopy (for $\tau_b = 0.15$) of a ray reflected from the surface, $\exp\{-0.15(\cos\theta_v)^{-1-z}\}$.

The illumination/viewing geometry parameter V_z is now specified as:

$$V_z(\theta_o,\theta_v) = \left(\frac{1}{\cos\theta_o}\right)^{1+z} + \left(\frac{1}{\cos\theta_v}\right)^{1+z}, \tag{4}$$

a function of solar zenith angle θ_o, view zenith angle θ_v, and the verticality parameter z. The exponent $1+z$ in equation 4 sums the effect of elongation of the path with increasing θ_v, $1/(\cos\theta_v)$, and the increase $(1/\cos\theta_v)^z$ in the optical thickness of plant elements (per unit of path-length) in the direction θ_v($z=0.0$ specifies the case of the spherical distribution). The Negev-to-Sinai ratio of bidirectional reflectances, R_n/R_e, is now given (for the same θ_o and θ_v in R_n and R_e) as:

$$R_n/R_e = \exp(-\tau_b V_z) \tag{5}$$

As we assume bare soil for the Sinai, the plant optical density (τ_b) inferred from this relation actually quantifies the difference in plant density between the Negev and the Sinai. As z increases, the derived values of τ_b become smaller, see table 2. Plant fraction of 18% as viewed from the zenith has been reported for the Negev, and of 4.5% for the Sinai, for a 13.5% difference (Q. Zhihao, personal communication,

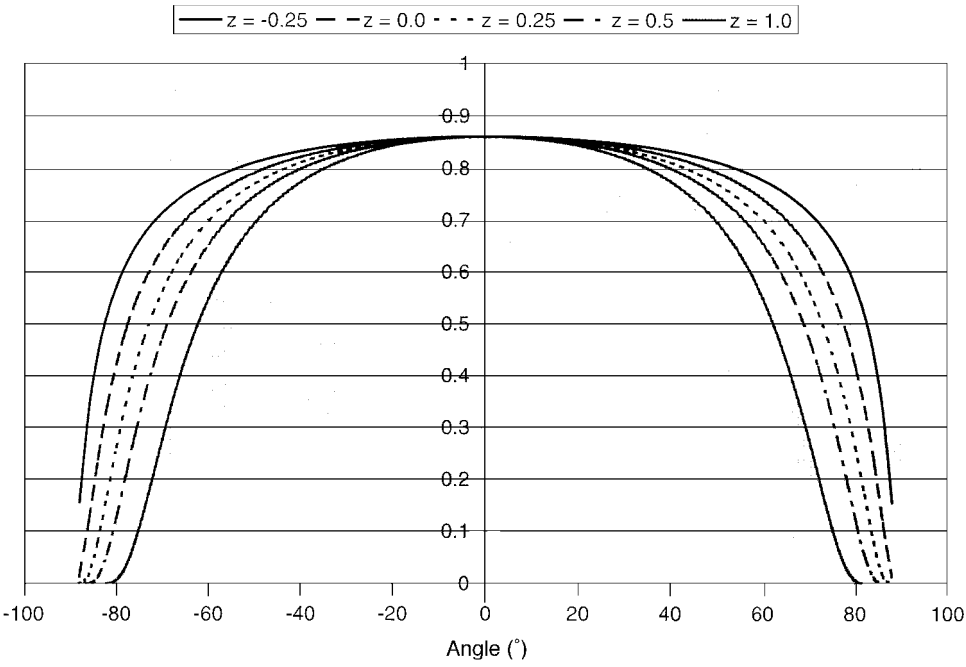

Figure 2. The cross-section for interception by the plant elements versus the zenith angle θ_v, for spherical ($z=0.0$) and non-spherical distributions, for z of -0.25, 0.00, 0.25, 0.50 and 1.00 as a section along the view zenith angle.

Table 2. Effect of the assumed tendency to vertical of desert scrub on the inferred optical thickness τ_b and on the Negev-to-Sinai albedo ratio $\rho_{az} = A_n/A_e$.

		Channel 1			Channel 2		
θ_o (°)	z	τ_b	σ	ρ_{az}	τ_b	σ	ρ_{az}
30°	−0.25	0.166	0.022	0.64	0.142	0.019	0.686
30°	0.00	0.159	0.022	0.627	0.136	0.019	0.669
30°	0.25	0.152	0.023	0.609	0.130	0.020	0.652
30°	0.50	0.145	0.024	0.592	0.124	0.021	0.635
30°	1.00	0.133	0.028	0.558	0.114	0.025	0.599
60°	−0.25	0.166	0.022	0.587	0.142	0.019	0.633
60°	0.00	0.159	0.022	0.548	0.136	0.019	0.596
60°	0.25	0.152	0.023	0.509	0.130	0.020	0.559
60°	0.50	0.145	0.024	0.470	0.124	0.021	0.521
60°	1.00	0.133	0.028	0.392	0.114	0.025	0.442

2000). These measurements would be consistent with z approaching 1.0 for which τ_b is 0.133 (channel 1, table 2).

We regard our new model, equation 4, as an improvement over the thin vertical-cylinders model (or, equivalently, vertical leaves randomly distributed in azimuth) for which obscuration and shadowing of the soil were expressed as dependent on tan θ_v and tan θ_o respectively (Otterman 1981b). Thus, at $\theta_v = \theta_o = 0.0°$ the plants become invisible, which indicates that the tangent-dependence model is not appropriate at small zenith angles.

The Negev-to-Sinai albedo ratio A_n/A_e is calculated for a specific θ_o by hemispheric integration:

$$\rho_{az}(\theta_o, z) = \frac{A_n}{A_e} = 2\int_0^{\pi/2} \exp\left\{-\tau_b\left[\left(\frac{1}{\cos\theta_o}\right)^{1+z} + \left(\frac{1}{\cos\theta_v}\right)^{1+z}\right]\right\} \cos\theta_v \sin\theta_v \, d\theta_v \quad (6)$$

As can be seen in table 2, an increased tendency to a vertical architecture (an increasing z), produces significantly lower ρ_{az} ratios (the impact is stronger) than for $z = 0.0$. Thus, for $z = 1.0$ at $\theta_o = 60°$, ρ_{az} is 0.39 in channel 1 and 0.44 in channel 2, as compared to 0.55 and 0.60 for $z = 0.0$.

5. Discussion and conclusions

The inversion from the bidirectional reflectance ratios, equation 1, yields the values of τ_b for the two AVHRR channels (channel 1, 0.63 μm band centre; channel 2, 0.85 μm centre). The τ_b values presented in table 1 and figure 1 are in the range 0.12 to 0.20 for channel 1 (visible). For channel 2 (solar infrared), τ_b has in each case a lower value, by about 0.01 to 0.03. These lower values are only to be expected: these dark stems of desert scrub (for a Negev ground photograph see Otterman (1996); for a photograph taken in the Sinai exclosure, where vegetation quickly recovered after fencing off, see Otterman and Tucker (1985)) do contain some green elements, which scatter rather than absorb in the infrared. Our assumption of absorbing plant elements is slightly less appropriate for channel 2 than for channel 1.

Evaluated from average values of τ_b, the Negev-to-Sinai spectral albedo ratios ρ_a are 0.63 and 0.55 in AVHRR channel 1, and 0.67 and 0.60 in channel 2, at solar zenith angles of 30° and 60°, respectively, when spherical distribution in the zenith angle of plant elements is assumed.

These ratios suggest severe climatic impact by overgrazing. In the Sinai, the high albedo reduces shortwave heat absorption, reducing therefore the daytime convection (see, for example, Berkofsky 1977). Weaker convection means lower probability of convective precipitation. The desert scrub in the Negev, on the other hand, not only reduces the surface albedo, but also by virtue of the low thermal inertia of the plant elements facilitates daytime heat transfer from the surface to the atmosphere (Otterman 1989).

Anthropogenic impact of overgrazing produces unstable, loose soil (as in the Sinai), essentially bare of vegetation, characterized by a high albedo, in contrast to a desert scrub surface in the protected areas. The control of grazing practices in the Negev (since 1948) produced such a low-albedo desert scrub surface. It appears that the desert scrub, after a rapid recovery when anthropogenic pressures are stopped, tends to persist at a more or less constant density (Otterman and Robinove 1982) consistent with climate and soil conditions. It appears these changes in the surface characteristics increased the convective rains in the region, which is the dominant type of precipitation early in the season (in October; Otterman *et al.* 1990). A pertinent measure for climate-change effects is the ratio Negev-to-Sinai of the spectral albedo (hemispheric reflectance). In this study, we note that the Negev-to-Sinai ratio A_n/A_e decreases (the effect of anthropogenic pressures is estimated as larger) when a stronger tendency to vertical canopy architecture is assumed (a positive z). Thus, for $z=1.0$, at $\theta_o=60°$ the z_a ratios become 0.39 in band 1 and 0.44 in band 2 (compared to 0.55 and 0.60 for $z=0.0$ quoted earlier in this section.

Our analysis here is somewhat simplistic, as we did not consider that the plants do reflect to some extent, even though they are much darker than the soil. In calculating the plant optical thickness τ_b, equation 1 or 5, we assume that the soil in the Negev has the same reflectance properties as the soil in the Sinai. Actually, the soil in the Negev could be slightly darker than the loose soil in the Sinai (Karnieli and Tsoar, 1995), and its anisotropy could be altered by stabilization. Still another simplification is that we consider the direct solar beam as the sole illumination source, neglecting the scattered sunlight (diffuse radiation). As our calculations of the ratio ρ_a depend on the direction of illumination (here the direct beam only at zenith angle θ_o), our neglect of the scattered sunlight (which effectively comes in at zenith angle of about 60°) may introduce appreciable inaccuracies. The importance of scattered sunlight as a source certainly increases with increasing θ_o but its evaluation depends on the scattering versus the absorbing properties of the atmosphere (Davé 1978), and specifically the single-scattering albedo of aerosols (which quantifies absorption versus scattering). The effects of contrast attenuation by the atmosphere are essentially removed by our atmospheric correction. Under clear sky conditions these effects are small for bright surfaces (see specific calculations for Sinai-Negev by Otterman and Fraser (1976)), but not necessarily negligible. We recommend a specific value of our verticality parameter, $z=0.5$, as appropriate for desert scrub since τ_b of 0.145 (in channel 1) fits quite well with the assessments from the zenith of the Negev plant cover. Our calculations, however, cannot be claimed to be truly quantitative. We note that the inferred value of τ_b, which apart from the surface albedo is an important parameter for assessing surface–atmosphere interactions (Otterman 1989), varies only in a narrow range with z.

The early analysis of the Sinai-to-Negev contrast (Otterman 1974, Otterman and Fraser 1976), in which the anisotropy of the surface reflectance was disregarded, seriously underestimated the effect of the anthropogenic impact. We conclude that plant architecture, which affects the reflection anisotropy, should be considered when evaluating the albedos of vegetated versus bare (impacted) surfaces. Uncertainty in the distribution of the leaf area as a function of the zenith angle can produce significant uncertainty in the albedo assessment. Multi-directional reflectance measurements over selected sites by an instrument such as the PARABOLA (Deering *et al.* 1993) should be conducted to provide information about the reflectance anisotropy; see the discussion of ground-truth measurements by Otterman *et al.* (1987) for determination of the desert scrub structure. This information should significantly enhance the value of satellite measurements.

5. Acknowledgments

Comments by D. Kimes and S. Sandmeier, NASA/GSFC, resulted in a significantly improved presentation of our model and of our conclusions.

References

Berkofsky, L., 1977, The relation between surface albedo and vertical velocity in a desert. *Contributions to Atmospheric Physics*, **50**, 312–320.

Blad, B. L., and Baker, D. G., 1972, Orientation and distribution of leaves within a soybean canopy. *Agronomy Journal*., **64**, 26–29.

Breece III, H. T., and Holmes, R. A., 1971, Bidirectional scattering characteristics of healthy green soybean and corn leaves *in vivo*. *Applied Optics*, **10**, 119–127.

Bunnik, N. J. J., 1978, The multispectral reflectance of shortwave radiation by agricultural crops in relation with their morphological and optical properties. *Mededelingen Landbouuwhogeschool, Wageningen, Nederland*, **78–1**, 175.

Colwell, J. E., 1974, Grass canopy spectral reflectance. *Proceedings of the 9th International Symposium on Remote Sensing of Environment,* April 15–19, Ann Arbor, Michigan, pp. 1061–1077.

Courel, M. F., Kandel, R. S., and Rasool, S. I., 1984, Surface albedo and the Sahel drought, *Nature*, **307**, 528–531.

Coulson, K. L., 1966, Effect of reflection properties of natural surfaces in aerial reconnaissance. *Applied Optics*, **5**, 905–917.

Coulson, K. L., and Reynolds, D. W., 1971, The spectral reflectance of natural surfaces. *Journal of Applied Meteorology,* **10**, 1285–1295.

Cracknell, A. P., 1997, *The Advanced Very High Resolution Radiometer (AVHRR)*, (London: Taylor and Francis).

Davé, J. V., 1978, Extensive datasets of the diffuse radiation in realistic atmospheric models with aerosols and common absorbing gases. *Solar Energy*, **21**, 361–369.

Deering, D. W., Eck, T. F., and Otterman, J., 1993, Bidirectional reflectances of selected desert surfaces and their three-parameter soil characterization. *Agricultural and Forest Meteorology*, **52**, 71–93.

Dregne, H. E., 1970, Arid Lands in Transition, *American Association for the Advancement of Science*, pp. 424.

Holben, B. N., Eck, T. F., Slutsker, I., Tanre, D., Buis, J. P., Setzer, A., Vermote, E., Reagan, J. A., Kaufman, Y. J., Nakajima, T., Lavenu, F., Jankowiak, I., and Smirnov, A., 1998, AERONET—A federated instrument network and data archive for aerosol characterization. *Remote Sensing of Environment*, **66**, 1–16.

Karnieli, A., and Tsoar, H., 1995, Satellite spectral reflectance of biogenic crust developed on desert dune sand along the Israel-Egypt border. *International Journal of Remote Sensing,* **16**, 369–374.

Kimes, D. S., and Sellers, P. J., 1985, Inferring hemispherical reflectance of the earth's surface for global energy budgets from remotely sensed nadir or directional radiance values. *Remote Sensing of Environment,* **18**, 205–223.

KOSLOWSKY, D., 1996, PhD Dissertation (in German). Institut fur Meteorologie der Freien Universitat Berlin, Met. Abh., Neue Folge, 9, D-12165 Berlin.

KOSLOWSKY, D., 1998, Improved long-term AVHRR reflectance and NDVI time series using empirically derived nadir correction factors, *Proceedings of the 9th Conference on Satellite Meteorology and Oceanography*, UNESCO, Paris, France, 25–29 May, AMS, Boston, MA, pp. 313–316.

OTTERMAN, J., 1974, Baring high-albedo soils by overgrazing: a hypothesized desertification mechanism. *Science*, **186**, 531–533.

OTTERMAN, J., 1981a, Satellite and field studies of man's impact on the surface in arid regions. *Tellus*, **33**, 68–77.

OTTERMAN, J., 1981b, Plane with protrusions as an atmospheric boundary. *Journal of Geophysical Research*, **86**, 6627–6630.

OTTERMAN, J., 1985, Bidirectional and hemispheric reflectivities of a bright soil plane and a sparse dark canopy. *International Journal of Remote Sensing*, **6**, 897–902.

OTTERMAN, J., 1989, Enhancement of surface-atmosphere fluxes by desert-fringe vegetation through reduction of surface albedo and of soil heat flux. *Theoretical and Applied Climatology*, **40**, 67–79.

OTTERMAN, J., 1996, Desert-scrub as the cause of reduced reflectances in protected versus impacted sandy arid areas. *International Journal of Remote Sensing*, **17**, 615–619.

OTTERMAN, J., and FRASER, R. S., 1976, Earth-atmosphere system and surface reflectivities in arid regions from Landsat MSS data. *Remote Sensing of Environment*, **5**, 247–266.

OTTERMAN, J., and ROBINOVE, J., 1982, Landsat monitoring of desert vegetation growth, 1972–1979, using a plant shadowing models. *Advances in Space Research,* **2**, 45–50.

OTTERMAN, J., and TUCKER, C. J., 1985, Satellite measurements of surface albedo and temperatures in semi-desert. *Journal of Climate and Applied Meteorology,* **24**, 228–235.

OTTERMAN, J., WAISEL, Y., and ROSENBERG, E., 1975, Western Negev and Sinai ecosystems: comparative study of vegetation, albedo and temperatures, *Agro-Ecosystems*, **2**, 47–52.

OTTERMAN, J., DEERING, D., ECK, T., and RINGROSE, S., 1987, Techniques of ground-truth measurements of desert-scrub structure. *Advances in Space Research*, **7**, 153–158.

OTTERMAN, J.,MANES, A., RUBIN, S., ALPERT, P., and STARR, D., 1990, An increase of early rains in southern Israel following land-use change? *Boundary-Layer Meteorology*, **53**, 333–351.

PINTY, B., VERSTRAETE, M. M., and DICKINSON, R. E., 1989, A physical model for predicting bidirectional reflectance over bare soil. *Remote Sensing of Environment*, **27**, 273–288.

RAO, N., and CHEN, J., 1996, Post-launch calibration of the visible and near-infrared channels of the AVHRR on the NOAA-14 spacecraft. *International Journal of Remote Sensing*, **17**, 2743–2747.

RAO, N., and CHEN, J., 1998, Revised post-launch calibration of channels 1 and 2 of the Advanced Very High Resolution Radiometer on board the NOAA-14 spacecraft. http://psbsgi1.nesdis.noaa.gov:8080/EBB/ml/niccal1.html.

VERMOTE, E., TANRE, D., DEUZE, J. L., HERMAN, M., and MORCETTE, J.-J., 1997, Second Simulation of the Satellite Signal in the Solar Spectrum (6S). *IEEE Transactions on Geoscience and Remote Sensing*, **35**, 675–685.